Brazilian Journal of Analytical Chemistry
Pre-publication – Accepted after peer review
doi: 10.30744/brjac.2179-3425.AR-44-2023

ARTICLE

Development of a Modified Electrode with N-doped Carbon Dots for Electrochemical Determination of 17α-ethinylestradiol

Brenda Rafaela Lima Freire, Michael Douglas Santos Monteiro, Jonatas de Oliveira Souza Silva, José Fernando de Macedo, Eliana Midori Sussuchi*

Grupo de Pesquisa em Sensores Eletroquímicos e nano(Materiais) – SEnM, Laboratório de Corrosão e Nanotecnologia – LCNT, Programa de Pós-Graduação em Química, Departamento de Química, Universidade Federal de Sergipe (UFS). Avenida Marechal Rondon Jardim s/n, São Cristóvão, SE, 49100-000, Brazil

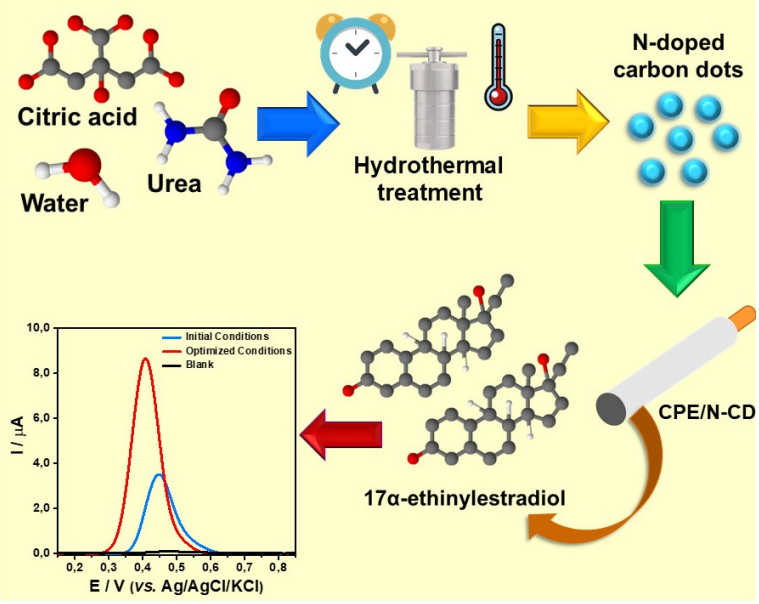

This work aims to develop a modified electrode with N-doped carbon dots (CPE/N-CD) for the voltammetric detection of 17α-ethinylestradiol (EE2) in solution. N-doped carbon dot nanoparticles (N-CD) were synthesized using citric acid and urea as the nitrogen source. The N-doped carbon dots were characterized by absorption and emission spectroscopy in the ultraviolet and visible regions, electronic absorption spectroscopy in the infrared region, and Raman spectroscopy, which showed evidence of the formation of the material. Electrochemical analyses were conducted utilizing differential pulse voltammetry (DPV). After optimization of electrochemical parameters, a calibration plot was produced for the sensor, demonstrating a linear range of 0.01 to 0.80 µmol L^{-1} (R^2 = 0.9969). Additionally, the sensor exhibited a detection limit (LOD) of 0.59 nmol L^{-1} and a quantification limit (LOQ) of 2.00 nmol L^{-1}. The studies on reproducibility and repeatability revealed RSDs of 1.63% and 3.61% respectively. The results obtained using CPE/N-CD indicate that the developed electrode exhibits excellent analytical performance, making it suitable for identifying and quantifying EE2 in solution.

Keywords: 17α-ethinylestradiol, hormones, voltammetry, nanomaterials, electrochemistry

INTRODUCTION

The increase in the global consumption of synthetic products has contributed to water pollution, with

Cite: Freire, B. R. L.; Monteiro, M. D. S.; Silva, J. O. S.; de Macedo, J. F.; Sussuchi, E. M. Development of a Modified Electrode with N-doped Carbon Dots for Electrochemical Determination of 17α-ethinylestradiol. *Braz. J. Anal. Chem.* (Forthcoming). http://dx.doi.org/10.30744/brjac.2179-3425.AR-44-2023

Submitted 26 May 2023, Resubmitted 27 July 2023, Accepted 05 August 2023, Available online August 2023.

several effects on human health and aquatic life. Among these compounds are micropollutants, which are contaminants at very low concentrations (ng-μg L^{-1}) that generate environmental problems.[1]

Micropollutants comprise a wide range of materials and compounds, including pesticides, pharmaceuticals, surfactants, and cosmetics. Within the realm of water quality, a notable presence of emerging contaminants, encompassing personal care products, medicinal substances, and endocrine-disrupting compounds (EDCs). These specific pollutants demonstrate a recurrent detection pattern in water samples. The United States Environmental Protection Agency (USEPA) defines EDCs as exogenous agents that interfere with the synthesis, secretion, transport, binding, action, or elimination of natural hormones from the body, which are responsible for maintaining homeostasis, reproduction, development, and/or behavior. These compounds are mainly represented by hormones, such as 17α-ethinylestradiol.[2-4]

17α-ethinylestradiol (EE2) is a synthetic hormone derived from the natural hormone estradiol, which is used in hormone replacement therapies, discontinuation of breastfeeding, and oral contraceptives. It is a pharmacologically active compound that can be introduced into aquatic bodies via excretion from humans and animals. Therefore, these compounds are released into rivers, affecting some of the living organisms that inhabit them, since the sewage treatment carried out at most stations is ineffective, mainly related to the regulation and scant inspection of environmental agencies.[5-8]

EE2 is highly persistent in the environment, with a half-life of 10 to 81 days, in addition to bioaccumulation and bioconcentration. In fish, exposure to this substance is frequently related to decreased fertility, changes in anatomy, induction of vitellogenin production, and feminization of male species.[9] The detection of 17α-ethinylestradiol can be carried out by an electrochemical route,[10] along with the application of nanomaterials that can improve electroanalytical strategies. Among nanomaterials, carbon dots (CD) are fluorescent carbonaceous nanoparticles that exhibit excellent properties such as good electrical conductivity and stability, low cost, and toxicity, since *in vitro* tests were performed on mice and they weren't affected negatively.[11-13]

Nanomaterials are commonly employed as electrode modifiers to improve the electrochemical signals.[14] Carbon dots exhibit better electrical properties than conductive polymers and are cheaper than noble transition metals.[15] In this context, Fu. *et.al*. developed a glassy carbon electrode modified with carbon dots doped with nitrogen for the detection of nitrogen peroxide and paracetamol, obtaining limits of detection of 157.0 nmol L^{-1} and 41.0 nmol L^{-1}, respectively.[16] Pudza *et. al*. developed a screen-printed carbon-modified electrode using fluorescent carbon dots derived from *tapioca* and gold nanoparticles (AuNPs) for sensing copper (Cu^{2+}), lead (Pb^{2+}), and cadmium (Cd^{2+}), resulting in detection limits of 0.0028, 0.0042, and 0.014 ppm, respectively.[17]

Because of environmental problems involving synthetic hormones, especially EE2, their identification, and monitoring are necessary. The present work proposes the development of a modified electrode with carbon dots for the determination of 17α-ethinylestradiol.

MATERIALS AND METHODS

Chemicals

CH_4N_2O (99,0%) was acquired from Vetec. NaOH (99.0%) was acquired from IMPEX. H_3BO_3 (99.9%) was acquired from Reagen. H_3PO_4 (85.0%) and NaH_2PO_4 (PA) were acquired from Synth. 17*α*-ethinylestradiol (98.0%, $C_{20}H_{24}O_2$) and graphite powder (99.9%, C) were acquired from Sigma-Aldrich. KBr (99.5%) was acquired from Merck. Citric acid (99.7%, $C_6H_8O_7$), ethanol (99.8%, C_2H_5OH), and Na_2HPO_4 (PA) were purchased from NEON. $K_3Fe(CN)_6$ (99.5%) was acquired from J.T. Barker. $K_4Fe(CN)_6.3H_2O$ trihydrate (99.0%) was acquired from Carlos Erba. Paraffin was acquired from GM Waxes. Hexane (99%, C_6H_{14}) was acquired from Dinâmica. The solutions were prepared utilizing ultrapure water obtained from a Milli-Q system (Merck Millipore). Phosphate (0.20 mol L^{-1}) and Britton-Robinson (B-R) (0.50 mol L^{-1}) buffer solutions were utilized, and the pH was adjusted using a solution of NaOH or HCl with a concentration of 3.00 mol L^{-1}. The EE2 stock solution (10.00 mmol L^{-1}) was prepared by dissolving the standard in ethanol, and less concentrated solutions were prepared by dilution.

Synthesis of N-doped carbon dots

N-doped carbon dot (N-CD) nanoparticles were synthesized using citric acid and urea as carbon and nitrogen sources, respectively, following the procedure proposed by Zhu et al.[18]: citric acid (1.0 g, 5 mmol) and urea (2.0 g, 33 mmol) were dissolved in 30.00 mL of ultrapure water, stirred for 30 min, and transferred into an 85 mL autoclave that was kept in hydrothermal treatment in an oven at 180 ºC for 8 h. The system was then cooled to room temperature, and a dark green solution was obtained and stored under refrigeration at 4 ºC.[18]

Sample characterizations

Ultraviolet-visible absorption spectra were obtained using a Varian Cary 100 Scan UV-Visible Spectrophotometer (UV-Vis), quartz cuvettes with a 1.0 cm optical path were used, and the ultrapure water was used as the reference solvent. Fourier transform infrared spectroscopy (FTIR) analyses were carried out utilizing a Shimadzu IRPrestige-21 model spectrometer, with a KBr pellet. Raman spectroscopy measurements were conducted using a confocal Raman microscope: Senterra II, manufactured by Bruker Optik GmbH, equipped with a 785 nm diode laser and a beam intensity of 100 mW. Emission spectroscopy analysis was performed using a JascoFP-8000 instrument in the 200–800 nm region. A quartz cuvette with a 1.00 cm optical path was used, where the N-CD suspension diluted in ultrapure water was deposited.

Electrochemical procedure

The analyses were performed using an AutoLab potentiostat/galvanostat model Autolab 100N, and the data obtained were processed using NOVA 2.1.5 software. A 15 mL electrochemical cell composed of three electrodes was used: the unmodified (CPE) or modified with N-doped carbon dots (CPE/N-CD) carbon paste electrode as the working electrode, platinum wire as the counter electrode, and Ag/AgCl/(3.00 mol L^{-1} KCl) as the reference electrode. The experiments were conducted in triplicate under ambient temperature and pressure.

The unmodified electrode (CPE) was obtained using a mixture of powdered graphite and paraffin in a ratio of 3:2 (w:w). The modified electrode (CPE/N-CD) was obtained maintaining the proportion of paraffin at 40.0%, while the amount of graphite powder was adjusted to the percentage of and N-doped carbon dot desired (2.5%, 5.0%, 7.5%, 15%, and 30%). The electrode constituents were weighed in a microtube, and the total mass of the paste was 200 mg. Next, 400 µL of hexane was added, and the microtube was placed in an ultrasound bath at 60 °C for 15 min to melt the paraffin. The system was then opened for 3 min and vortexed for 1 min. The walls of the microtubes were then washed with hexane (200 µL). After complete solvent evaporation in an ultrasonic bath, the paste was transferred into a Petri dish and subjected to thermal treatment at 60 ºC for 12 hours in an oven.

A consistent paste was prepared and placed inside a polypropylene tube with an inner diameter of 4.8 mm. Electrical contact was achieved by inserting a copper wire with a diameter of 3.0 mm. After each analysis, the electrode surface was manually polished against filter paper to renew it.

RESULTS AND DISCUSSION

Characterization of the N-doped carbon dots

The FTIR spectra (Figure 1a) show an intense O-H stretching band at 3645 cm^{-1} for the citric acid sample. In the urea sample, an N-H stretching band can be identified at 3363 cm^{-1}, and in the same region in the N-CD sample, the N-H and O-H stretching bands appear superposed, suggesting the existence of two bonds in the N-CDs, which can be attributed to the precursors and water uptake by the N-CDs. It was observed that in the region at approximately 1719 cm^{-1}, the C=O stretching bands appeared in the precursors, and the sample of N-CD and the C-N stretching band at 1391 cm^{-1}, which suggests that the nitrogen-derived urea was well incorporated into the structure of N-CD.[19-21]

The Raman spectrum of N-CD (Figure 1b) shows that the D band at 1254 cm^{-1} can be attributed to the presence of sp^2 and sp^3 hybridized carbon-carbon bonds, indicating structural disorder or defects

in the N-CD. The G band at 1593 cm^{-1} indicates the presence of graphitic carbon, that is, conjugated C=C bonds. The absorption spectra obtained in the range of 400-800 nm are shown in Figure 1c. The presence of absorption bands at 230 nm is attributed to π-π* transitions, and that at 330 nm is attributed to n-π* transitions arising from the C=O bond of N-CD. The n-π* transitions are of great importance in N-CDs because they are related to doping and functionalization of the material surface. The π-π* band can be assigned to the charge transfer of a C=C conjugated bond.[22,23] The emission spectrum (Figure 1d) shows that the N-CD sample excited at different wavelengths in the range of 320 and 380 nm, presents its maximum peak at 437 nm under an excitation wavelength of 350 nm. This result indicates that the N-CD did not display any emission pattern that varied with the level of excitation, which can be attributed to the composition of the nanomaterial.[24]

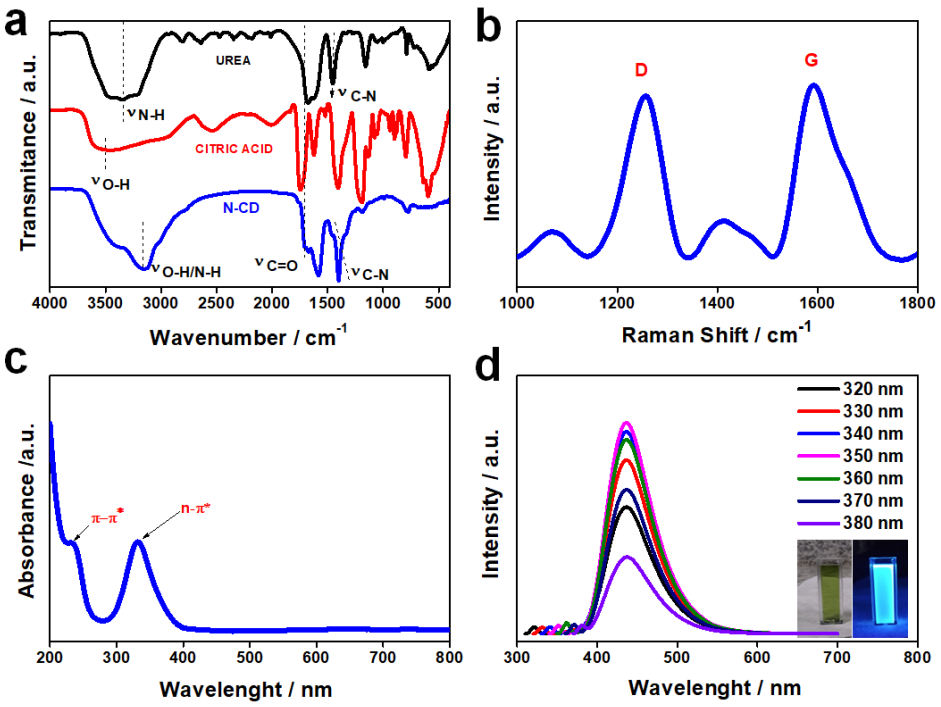

Figure 1. a) FTIR spectra of urea, citric acid, and N-CD. b) Raman spectrum of N-CD. c) Absorption spectra of N-CD. d) Emission spectra of N-CD.

Electrochemical performance of CPE/N-CD

The analyses initially aimed to evaluate the electrochemical behavior of EE2 using CPE and CPE/N-CD containing 11:1:8 (w:w:w) proportion of the graphite powder, mineral oil and N-CD modifier as the working electrode. Anodic differential pulse voltammograms were measured using EE2 10.0 μmol L^{-1} of in the presence of the supporting electrolyte (blank).

The results (Figure 2a) show that the anodic peak of EE2 can be seen between +0.35 and +0.55 V (*vs.* Ag/AgCl) for both electrodes. The current intensity of CPE/N-CD was approximately 36.5% higher than that of CPE. This can be attributed the enhancement of the interaction with the analyte by the surface groups contained in the N-CD, which corroborated with the greater detectability presented by the electrode.

Influence of parameters optimization

The influence of the supporting electrolyte was studied using, phosphate and B-R buffers (pH = 7.00), and the obtained data are shown in Figure 2b. It can be observed that there is no significant difference between the oxidation signals obtained in the two electrolytes, with an increase in the current intensity

in the B-R buffer of only 13.2% for the phosphate buffer. Thus, the electrolyte chosen was B-R buffer because of its high buffering capacity over a wide pH range (2.0 – 12.0).

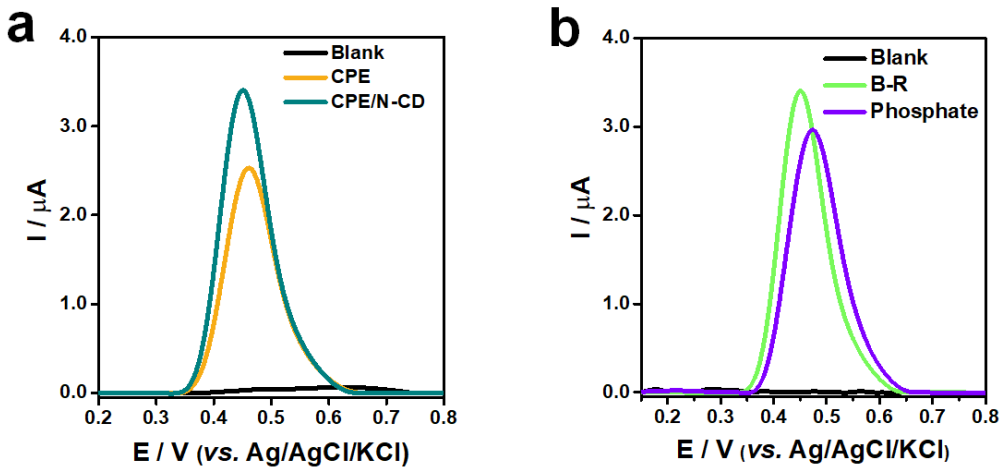

Figure 2. (a) Comparison between CPE and CPE/N-CD electrodes. (b) Anodic differential pulse voltammograms using CPE and CPE/N-CD 5% in Britton-Robinson and phosphate (pH 7.0) buffers, scan rate (v) = 20 mV s^{-1}, pulse amplitude (PA) = 100 mV, pulse time (t) = 10 ms, accumulation time (AT) = 60 s for detection of (EE2 10.0 µmol L^{-1}).

The pH of the electrolyte solution is one of the most influential parameters in the study of the electrochemical behavior of species, particularly the oxidation/reduction potentials. The study of this influence was carried out with the previously chosen B-R buffer, in the pH range of 2.0 – 10.0. From the results in Figure 3a, it can be observed that as the pH increased, the oxidation potential of EE2 shifted to less positive values. This is most evident in Figure 3b, which shows the linear relationship of the peak anodic current with the pH and potential. The slope of the linear equation (R^2 = 0.9974) was 59.7 mV ΔpH^{-1} which is close to the Nernst coefficient (59.2 ΔpH^{-1}) suggesting that the number of electrons involved in the oxidation process is equal to the number of protons (Figure 3c.).[24-25] The pH chosen for further study was 8.0. Although the peak width was slightly larger than that at pH 7.0 and 9.0, it has a potential less positive, closest to the physiological pH which favors EE2 oxidation with less energy spent in the process.

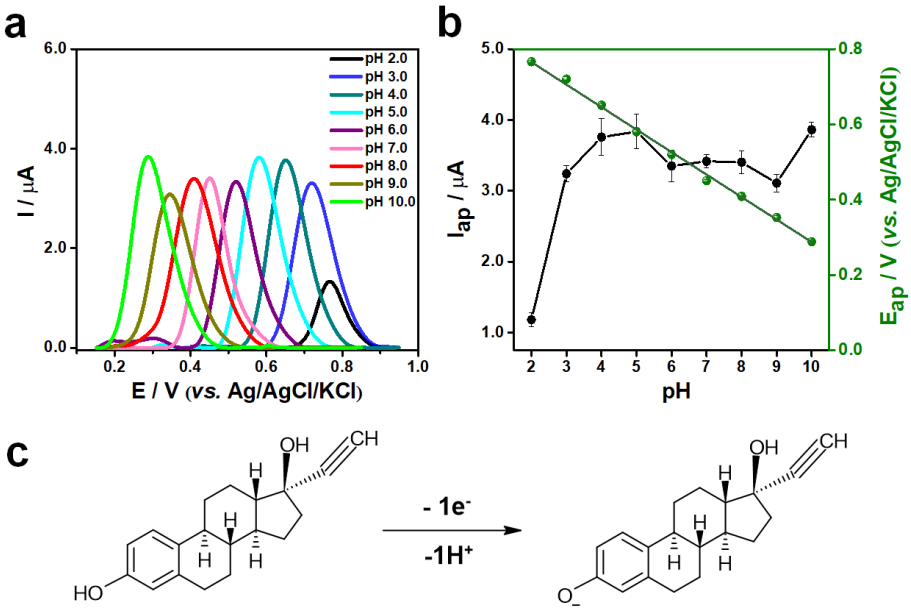

Figure 3. a) Anodic differential pulse voltammograms using CPE/N-CD 5% in B-R buffer pH (2.0 – 10.0, ν = 20 mV s^{-1}, PA = 100 mV, t = 10 ms, AT = 60 s) for detection of EE2 10.0 µmol L^{-1}. b) Variations in the potential and current intensity as a function of pH. c) Suggested oxidation mechanism of EE2.[26]

The study of accumulation time was carried out between 0 and 600 s. The graph in Figure 4a shows that the accumulation technique does not offer advantages in terms of current intensity. It is evident that as the contact time of CPE/N-CD with the analyte in the electrolytic medium increased, lower signal intensity values were obtained. This indicates that there is a possible saturation of the electrode surface at times longer than 30 s. Therefore, we decided to proceed with the optimization without using an accumulation technique. The results offer the advantage of shorter and more dynamic analysis times.

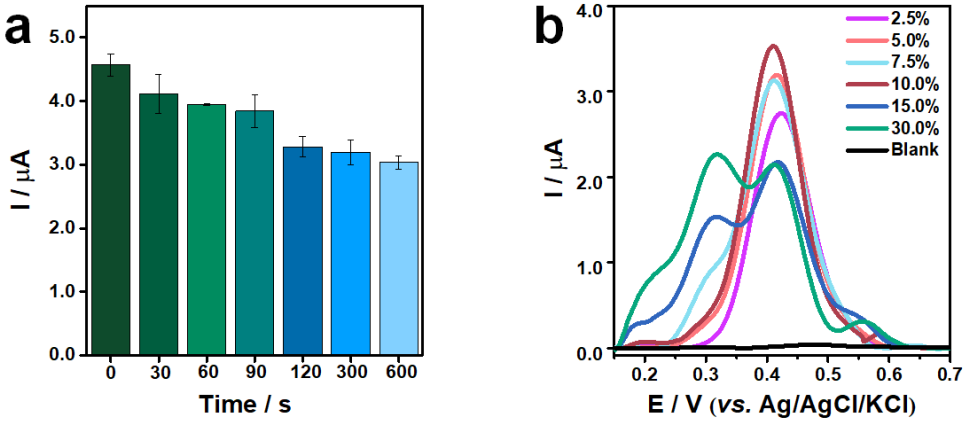

Figure 4. a) Variation in anodic peak current intensity with accumulation time. b) Anodic differential pulse voltammograms using different proportions of N-CD modifier (2.5, 5.0, 7.5, 10.0, 15.0, and 30.0%) in Britton- Robinson buffer (pH 8.0), ν = 20 mV s^{-1}, PA = 100 mV, and t = 10 ms for detection of EE2 10.0 µmol L^{-1}.

The influence of the proportion of the N-CD modifier on the anodic peak intensity of EE2 was studied to analyze the interaction of the modifier with the analyte. The voltammograms in Figure 4b demonstrate that an increase in the proportion of the modifier in the electrode composition by up to 10% made it possible to increase the anodic peak current intensity related to EE2. At 7.5, 15, and 30% of the modifier, the appearance of an anodic peak adjacent to the EE2 peak is visible. This may have been caused by the leaching of the modifier into the solution because, during the analysis, the supporting electrolyte turned from colorless to green, resulting in an N-CD oxidation process at that potential.[27] In addition to the lower intensities, large amounts of modifiers did not produce good analytical results for EE2. Therefore, the proportion chosen for follow-up experiments was 10%.

The scan rate plays a key role in the voltammetric analysis as it controls the speed at which the applied potential is scanned. Therefore, high scan rates tend to decrease the size of the diffuse layer and cause an increase in peak intensity.[28] In this study, voltammetric analyses were performed at different scan rates in the range of 5.0 to 30 mV s^{-1} to analyze their effect on the analytical signal of EE2. The voltammograms contained in Figure 5a shows an increase in the scan rate, providing an increase in the anodic peak intensities and width at half height ($W_{1/2}$). However, the scan rate of 30 mV s^{-1}, despite having an intense peak compared to the others, presented a significant $W_{1/2}$ of the peak, making its choice unfeasible owing to the low selectivity. A scan rate of 20 mV s^{-1} was chosen to follow the other optimizations because it had a smaller $W_{1/2}$ and still had a high anodic peak intensity.

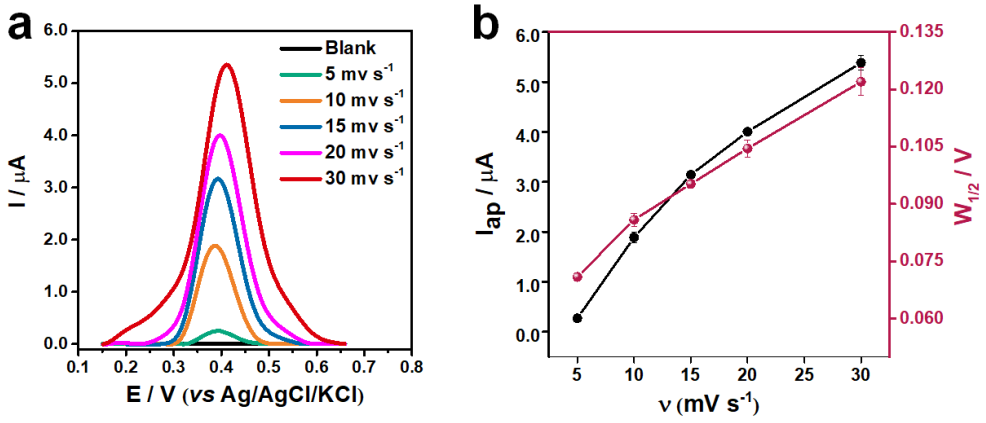

Figure 5. a) Anodic differential pulse voltammograms using CPE/N-CD 10% in Britton-Robinson buffer (pH 8.0, v = 5.0, 10.0, 15.0, 20.0, 30.0 mV s^{-1}, PA = 100 mV, and t = 10 ms) for detection of EE2 10 µmol L^{-1}. b) Current intensity variation and $W_{1/2}$ as a function of scan rate.

Different pulse amplitudes in the range of 5-125 mV were evaluated to study the relationship of this variation with electrode selectivity and EE2 oxidation intensity. Considering the voltammograms in Figure 6a, an increase in the intensity of the anodic peak was noticeable as the pulse amplitude increased. For values above 100 mV, there was a decrease in $W_{1/2}$ (Figure 6b) and intensity with the highest amplitude value and the potential shift to lower values, favoring the detection of the analyte under better conditions. Therefore, an amplitude of 100 mV was chosen for further experiments.

Pulse time optimization occurred at intervals of 2.5 and 50 ms. The data in Figure 6c show an increase in the anodic peak current with a decrease in the pulse time. In Figure 6d, it is noticeable that $W_{1/2}$ decreases with increasing time, but this is not a significant difference. The time of 2.5 ms presented higher current intensity. Therefore, this was chosen for further experiments.

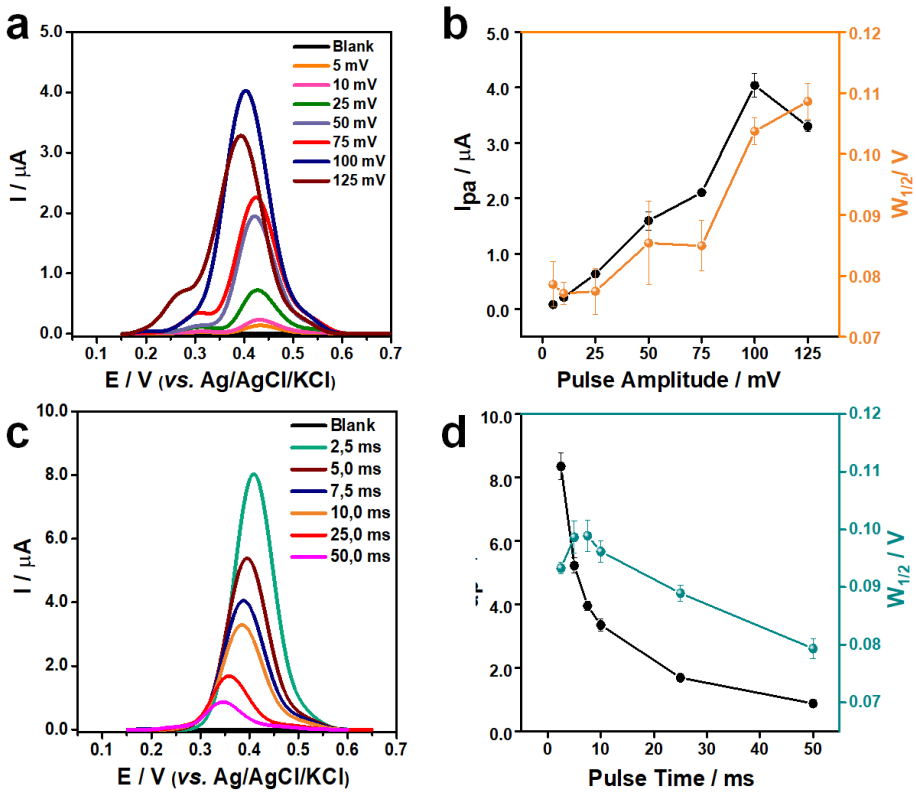

Figure 6. a) Anodic differential pulse voltammograms using CPE/N-CD 10% in Britton-Robinson buffer pH 8.0, v = 20 mV s^{-1}, PA = 5, 10, 25, 50, 75, 100, 125 mV, t = 10 ms for detection of 10.00 µmol L^{-1} of EE2; b) Variation of current intensity and $W_{1/2}$ as a function of pulse amplitude; c) Anodic differential pulse voltammograms using CPE/N-CD 10% in Britton- Robinson buffer pH 8.0, v = 20.0 mV s^{-1}, PA = 100.0 mV, t = 2.5; 5.0; 7.5; 10.0; 25.0; 50.0 ms for detection of 10.00 µmol L^{-1} of EE2; d) Variation of current intensity and $W_{1/2}$ as a function of pulse time.

The difference between the current intensities with CPE/N-CD under initial and optimal conditions represented a gain in the analytical signal of 145.4%, which reinforces the importance of conducting previous studies on technical and instrumental variables. Outlined below (Table I) is a condensed overview of the parameters studied and optimized to obtain the analytical curve.

Table I. Optimized conditions obtained for the developed methodology

Parameters		Optimal conditions
Measurement medium	Support Electrolyte	B-R buffer
	pH	8.0
Analytical Methodology	Accumulation time	None
	Modifier	10.0% (w/w)
Technique parameters	Pulse time	2.5 ms
	Pulse amplitude	100 mV
	Scan rate	20.0 mV s^{-1}

Analytical curve

Analytical curves were obtained in the presence of different concentrations of EE2. The linear behavior was observed between 0.01 and 0.80 µmol L^{-1}. The limits of detection (LOD= 3(Sd/b)) and quantification (LOQ= 10 (Sd/b)) were calculated, and the standard deviation (Sd) of the blank measurements (n= 3), as well as the slope of the linear equation (b), were estimated. The voltammograms in Figure 8a shows that the increase in the intensity of the oxidation peaks was proportional to the concentration of the EE2 solution. In Figure 8b, it is possible to observe the linear behavior with R^2 = 0.9969, resulting in the following equation: I_{EE2} = 6.38.10^{-8} + 0,75 X C_{EE2} The LOD was 0.59 nmol L^{-1} and the LOQ was 1.99 nmol L^{-1}.

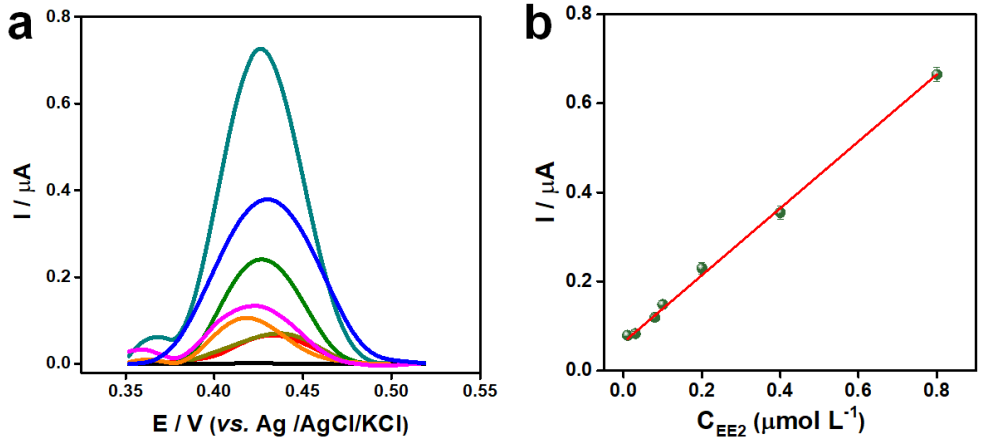

Figure 7. a) Differential pulse voltammograms for the CPE/N-CD 10% electrode in the concentration range of 0.01 - 0.80 µmol L^{-1} Britton-Robinson buffer (pH 8.0, PA = 100 mV, t = 2.5 ms, v = 20.0 mV s^{-1}). b) Calibration curve from the EE2 anodic peak currents.

All figures of merit are shown in Table II with a comparison between the electrode from this study and other sensors reported in the literature for the determination of EE2. The analytical curve showed favorable results for the detection of EE2 using CPE/N-CD. Through a comparison with other sensors in the literature, it is possible to visualize that the electrode obtained in this work has similar sensitivities, considering the detection limit and concentration range of the analytical curve. It is important to emphasize that the composition of CPE/N-CD is simple, and its modifier is easy to obtain. Also, the LD value of the method is low compared to the studies presented in the literature, which reinforces the ability to contribute to studies of electroanalytical methods for the detection of EE2.

Table II. Comparison between the results obtained with CPE/N-CD and those reported in the literature

Electrodes	LDR / µmol L^{-1}	LOD / nmol L^{-1}	Ref.
Au/Fe_3O_4@TA/MWNT/GCE	0.01 – 120.00	3.30	29
(mag@MIP)-GQDs-FG-F/SPE	0.01 - 2,50	2.60	30
PVP/Chi/rGO_Laccase	0.00025 – 0.02	0.00015	31
CPE/CPB	0.05 – 20.00	30.00	32
ErGOAs15%	0.04 – 8.28	6.79	33
CPE/N-CD	0.01 – 0.08	0.59	a

LDR: Linear Dynamic Range; LOD: Limit of detection; Au/Fe_3O_4@TA/MWNT/GCE: multiwall carbon nanotubes and magnetic nanoparticles functionalized with tannic acid and Au nanoparticles; (mag@MIP)-GQDs-FG-NF/SPE: Electrode modified with functionalized graphene, graphene quantum dots and magnetic nanoparticles coated with molecularly imprinted polymers; CPE/CPB: Carbon Black Modified Electrode; ErGOAs15%: modified carbon paste electrode with reduced graphene oxide; a: Present work.

Reproducibility assessments were conducted by obtaining six electrodes on different days under conditions. Anodic differential pulse measurements were taken for each electrode in the presence of EE2 10 μmol L^{-1}, revealing a relative standard deviation (RSD) of 1.61%. Repeatability tests were conducted using CPE/N-CD with a concentration of 10 μmol L^{-1} EE2 under optimized conditions. The tests involved performing six measurements, and the anodic peak current exhibited a relative standard deviation of 3.61%. To ensure consistency, the electrode surface was renewed after each measurement. These outcomes demonstrate the reliable and consistent performance of the developed sensor, affirming the method's robustness.

CONCLUSIONS

The CPE/N-CD electrode demonstrated a higher detection sensitivity of EE2 concerning CPE, and optimization of the parameters showed a greater analytical response to the analyte. The analytical curve provided information regarding the linearity of the electrochemical signal in the concentration range of 0.01 – 0.80 μmol L^{-1}, and low detection and quantification limits as well as good relative standard deviations were observed. Thus, the electrode modified with N-CD had good electrochemical characteristics for the determination of the analyte in aqueous solutions.

Conflicts of interest

We hereby affirm that there are no conflicts of interest related to the information presented in this article.

Acknowledgements

The authors would like to thank PETROBRAS for providing the infrastructure and "Centro de Laboratórios de Química Multiusuários" (CLQM) from the Federal University of Sergipe (UFS) for their support in the analysis. This work was supported by the "Conselho Nacional de Desenvolvimento Científico e Tecnológico" (CNPq); "Coordenação de Aperfeiçoamento de Pessoal de Nível Superior" (CAPES) and "Fundação de Apoio à Pesquisa e à Inovação Tecnológica do Estado de Sergipe" (FAPITEC).

REFERENCES

(1) Margot, J.; Rossi, L.; Barry, D. A.; Holliger, C. A Review of the Fate of Micropollutants in Wastewater Treatment Plants. *WIREs Water* **2015**, *2* (5), 457–487. https://doi.org/10.1002/wat2.1090

(2) Kim, M.-K.; Zoh, K.-D. Occurrence and Removals of Micropollutants in Water Environment. *Environ. Eng. Res.* **2016**, *21* (4), 319–332. https://doi.org/10.4491/eer.2016.115

(3) United States Environmental Protection Agency (USEPA). *Special Report on Environmental Endocrine Disruption: An Effects Assessment and Analysis*, EPA/630/R-96/012. USEPA, Washington D.C, February 1997.

(4) Zhang, C.; Li, Y.; Wang, C.; Niu, L.; Cai, W. Occurrence of Endocrine Disrupting Compounds in Aqueous Environment and Their Bacterial Degradation: A Review. *Crit. Rev. Environ. Sci. Technol.* **2016**, *46* (1), 1–59. https://doi.org/10.1080/10643389.2015.1061881

(5) Nunes, C. N.; Pauluk, L. E.; Felsner, M. L.; dos Anjos, V. E.; Quináia, S. P. Rapid Screening Method for Detecting Ethinyl Estradiol in Natural Water Employing Voltammetry. *J. Anal. Methods. Chem.* **2016**, *2016*, 1–7. https://doi.org/10.1155/2016/3217080

(6) Martínez, N. A.; Pereira, S. V.; Bertolino, F. A.; Schneider, R. J.; Messina, G. A.; Raba, J. Electrochemical Detection of a Powerful Estrogenic Endocrine Disruptor: Ethinylestradiol in Water Samples through Bioseparation Procedure. *Anal. Chim. Acta* **2012**, *723*, 27–32. https://doi.org/10.1016/j.aca.2012.02.033

(7) Bolong, N.; Ismail, A. F.; Salim, M. R.; Matsuura, T. A Review of the Effects of Emerging Contaminants in Wastewater and Options for Their Removal. *Desalination* **2009**, 239 (1–3), 229–246. https://doi.org/10.1016/j.desal.2008.03.020

(8) Schug, T. T.; Janesick, A.; Blumberg, B.; Heindel, J. J. Endocrine Disrupting Chemicals and Disease Susceptibility. *J. Steroid Biochem. Mol. Biol.* **2011**, *127* (3–5), 204–215. https://doi.org/10.1016/j.jsbmb.2011.08.007
(9) Daniel, M. D. S.; De Lima, E. C. Determinação Simultânea de Estriol, β-Estradiol, 17α–etinilestradiol e Estrona Empregando-Se Extração em Fase Sólida (SPE) e Cromatografia Líquida de Alta Eficiência (HPLC). *Rev. Ambient. Água* **2014**, *9* (4), 688–695. https://doi.org/10.4136/ambi-agua.1346
(10) Triviño, J. J.; Gómez, M.; Valenzuela, J.; Vera, A.; Arancibia, V. Determination of a Natural (17β-Estradiol) and a Synthetic (17α-Ethinylestradiol) Hormones in Pharmaceutical Formulations and Urine by Adsorptive Stripping Voltammetry. *Sensors and Actuators B: Chemical* **2019**, *297*, 126728. https://doi.org/10.1016/j.snb.2019.126728
(11) da Silva, J. C. G. E.; Gonçalves, H. M. R. Analytical and Bioanalytical Applications of Carbon Dots. *TrAC, Trends Anal. Chem.* **2011**, *30* (8), 1327–1336. https://doi.org/10.1016/j.trac.2011.04.009
(12) Xu, X.; Ray, R.; Gu, Y.; Ploehn, H. J.; Gearheart, L.; Raker, K.; Scrivens, W. A. Electrophoretic Analysis and Purification of Fluorescent Single-Walled Carbon Nanotube Fragments. *J. Am. Chem. Soc.* **2004**, *126* (40), 12736–12737. https://doi.org/10.1021/ja040082h
(13) Zheng, X. T.; Ananthanarayanan, A.; Luo, K. Q.; Chen, P. Glowing Graphene Quantum Dots and Carbon Dots: Properties, Syntheses, and Biological Applications. *Small* **2015**, *11* (14), 1620–1636. https://doi.org/10.1002/smll.201402648
(14) Bonet-San-Emeterio, M.; Algarra, M.; Petković, M.; del Valle, M. Modification of Electrodes with N-and S-Doped Carbon Dots. Evaluation of the Electrochemical Response. *Talanta* **2020**, *212*, 120806. https://doi.org/10.1016/j.talanta.2020.120806
(15) Lin, X.; Xiong, M.; Zhang, J.; He, C.; Ma, X.; Zhang, H.; Kuang, Y.; Yang, M.; Huang, Q. Carbon Dots Based on Natural Resources: Synthesis and Applications in Sensors. *Microchem. J.* **2021**, *160*, 105604. https://doi.org/10.1016/j.microc.2020.105604
(16) Fu, L.; Wang, A.; Lai, G.; Lin, C.-T.; Yu, J.; Yu, A.; Liu, Z.; Xie, K.; Su, W. A Glassy Carbon Electrode Modified with N-Doped Carbon Dots for Improved Detection of Hydrogen Peroxide and Paracetamol. *Microchim. Acta* **2018**, *185* (2), 87. https://doi.org/10.1007/s00604-017-2646-9
(17) Pudza, M. Y.; Abidin, Z. Z.; Abdul-Rashid, S.; Yasin, F. M.; Noor, A. S. M.; Abdullah, J. Selective and Simultaneous Detection of Cadmium, Lead, and Copper by Tapioca-Derived Carbon Dot–Modified Electrode. *Environ. Sci. Pollut. Res.* **2020**, *27* (12), 13315–13324. https://doi.org/10.1007/s11356-020-07695-7
(18) Zhu, J.; Bai, X.; Bai, J.; Pan, G.; Zhu, Y.; Zhai, Y.; Shao, H.; Chen, X.; Dong, B.; Zhang, H.; Song, H. Emitting Color Tunable Carbon Dots by Adjusting Solvent towards Light-Emitting Devices. *Nanotechnology* **2018**, *29* (8), 085705. https://doi.org/10.1088/1361-6528/aaa321
(19) Strauss, V.; Wang, H.; Delacroix, S.; Ledendecker, M.; Wessig, P. Carbon Nanodots Revised: The Thermal Citric Acid/Urea Reaction. *Chem. Sci.* **2020**, *11* (31), 8256–8266. https://doi.org/10.1039/D0SC01605E
(20) Lai, X.; Liu, C.; He, H.; Li, J.; Wang, L.; Long, Q.; Zhang, P.; Huang, Y. Hydrothermal Synthesis and Characterization of Nitrogen-Doped Fluorescent Carbon Quantum Dots from Citric Acid and Urea. *Ferroelectrics* **2020**, *566* (1), 116–123. https://doi.org/10.1080/00150193.2020.1762435
(21) Gu, S.; Hsieh, C.-T.; Yuan, C.-Y.; Gandomi, Y. A.; Chang, J.-K.; Fu, C.-C.; Yang, J.-W.; Juang, R.-S. Fluorescence of Functionalized Graphene Quantum Dots Prepared from Infrared-Assisted Pyrolysis of Citric Acid and Urea. *J. Lumin.* **2020**, *217*, 116774. https://doi.org/10.1016/j.jlumin.2019.116774
(22) Sudolská, M.; Dubecký, M.; Sarkar, S.; Reckmeier, C. J.; Zbořil, R.; Rogach, A. L.; Otyepka, M. Nature of Absorption Bands in Oxygen-Functionalized Graphitic Carbon Dots. *J. Phys. Chem. C* **2015**, *119* (23), 13369–13373. https://doi.org/10.1021/acs.jpcc.5b04080
(23) Penner, M. H. Ultraviolet, Visible, and Fluorescence Spectroscopy. In: Nielsen, S. S. (Ed). *Food Analysis*, pp 89-106. Food Science Text Series. Springer, Cham, 2017. https://doi.org/10.1007/978-3-319-45776-5_7

(24) Silva, J. O. S.; Sant'Anna, M. V. S.; Gevaerd, A.; Lima, J. B. S.; Monteiro, M. D. S.; Carvalho, S. W. M. M.; Sussuchi, E. M. A Novel Carbon Nitride Nanosheets-based Electrochemical Sensor for Determination of Hydroxychloroquine in Pharmaceutical Formulation and Synthetic Urine Samples. *Electroanalysis* **2021**, *33* (10), 2152–2160. https://doi.org/10.1002/elan.202100170

(25) Sant'Anna, M. V. S.; Carvalho, S. W. M. M.; Gevaerd, A.; Silva, J. O. S.; Santos, E.; Carregosa, I. S. C.; Wisniewski, A.; Marcolino-Junior, L. H.; Bergamini, M. F.; Sussuchi, E. M. Electrochemical Sensor Based on Biochar and Reduced Graphene Oxide Nanocomposite for Carbendazim Determination. *Talanta* **2020**, *220*, 121334. https://doi.org/10.1016/j.talanta.2020.121334

(26) Coelho, M. K. L.; da Silva, D. N.; Pereira, A. C. Development of Electrochemical Sensor Based on Carbonaceal and Metal Phthalocyanines Materials for Determination of Ethinyl Estradiol. *Chemosensors* **2019**, *7* (3), 32. https://doi.org/10.3390/chemosensors7030032

(27) Vercelli, B.; Donnini, R.; Ghezzi, F.; Sansonetti, A.; Giovanella, U.; La Ferla, B. Nitrogen-Doped Carbon Quantum Dots Obtained Hydrothermally from Citric Acid and Urea: The Role of the Specific Nitrogen Centers in Their Electrochemical and Optical Responses. *Electrochim Acta* **2021**, *387*, 138557. https://doi.org/10.1016/j.electacta.2021.138557

(28) Elgrishi, N.; Rountree, K. J.; McCarthy, B. D.; Rountree, E. S.; Eisenhart, T. T.; Dempsey, J. L. A Practical Beginner's Guide to Cyclic Voltammetry. *J. Chem. Educ.* **2018**, *95* (2), 197–206. https://doi.org/10.1021/acs.jchemed.7b00361

(29) Nodehi, M.; Baghayeri, M.; Ansari, R.; Veisi, H. Electrochemical Quantification of 17α – Ethinylestradiol in Biological Samples Using a Au/Fe3O4@TA/MWNT/GCE Sensor. *Mater. Chem. Phys.* **2020**, *244*, 122687. https://doi.org/10.1016/j.matchemphys.2020.122687

(30) Santos, A. M.; Wong, A.; Prado, T. M.; Fava, E. L.; Fatibello-Filho, O.; Sotomayor, M. D. P. T.; Moraes, F. C. Voltammetric Determination of Ethinylestradiol Using Screen-Printed Electrode Modified with Functionalized Graphene, Graphene Quantum Dots and Magnetic Nanoparticles Coated with Molecularly Imprinted Polymers. *Talanta* **2021**, *224*, 121804. https://doi.org/10.1016/j.talanta.2020.121804

(31) Pavinatto, A.; Mercante, L. A.; Facure, M. H. M.; Pena, R. B.; Sanfelice, R. C.; Mattoso, L. H. C.; Correa, D. S. Ultrasensitive Biosensor Based on Polyvinylpyrrolidone/Chitosan/Reduced Graphene Oxide Electrospun Nanofibers for 17α – Ethinylestradiol Electrochemical Detection. *Appl. Surf. Sci.* **2018**, *458*, 431–437. https://doi.org/10.1016/j.apsusc.2018.07.035

(32) Smajdor, J.; Piech, R.; Pięk, M.; Paczosa-Bator, B. Sensitive Voltammetric Determination of Ethinyl Estradiol on Carbon Black Modified Electrode. *J. Electrochem. Soc*. **2017**, *164* (13), H885–H889. https://doi.org/10.1149/2.0851713jes

(33) Monteiro, M. D. S.; Sant'Anna, M. V. S.; Santos Junior, J. C.; Macedo, J. F.; Alves, A. A. C.; de Oliveira S. Silva, J.; Gimenez, I. F.; Sussuchi, E. M. Reduced Graphene Oxide-based Sensor for 17α-Ehinylestradiol Voltammetric Determination in Wastewater, Tablets and Synthetic Urine Samples. *Electroanalysis* **2022**, *34* (9), 1422–1430. https://doi.org/10.1002/elan.202100500